Supporting Information

Heteroanionic [VOxS4-x] Groups: Tetrahedral Units with Large Bire-fringence for Mid-infrared Nonlinear Optical Crystals

Shengzi Zhang,[†ab] Linfeng Dong,[†ad] Bohui Xu,[ad] Huige Chen,[ad] Hao Huo,[ad] Fei Liang, [a] Rui Wu,[c] Pifu Gong,*[a] and Zheshuai Lin*[ad]

Abstract: Tetrahedral groups can possess wide bandgap and large second harmonic generation (SHG) response in nonlinear optical (NLO) materials, but they usually exhibit small optical birefringence owing to low structural anisotropy, which would deteriorate the NLO performance. Herein the [VO_xS_{4-x}] (x = 0 - 4) tetrahedra that combine V^{5+} cation with oxygen-sulfur hybrid anions are highlighted as a type of good structural groups to overcome the above problem. We systematically investigate the optical and NLO properties of all reported V^{5+}-based thiovanadates theoretically. The calculated results reveal the largest birefringence (~0.37 in $Ba_5V_2O_4S_8$) among the pure tetrahedra-based compounds and indicate the potential of [VO_xS_{4-x}] units in enhancing birefringence and well-balanced NLO performance suitable for mid-infrared (mid-IR) region. Furthermore, Na_3VOS_3 in this family is selected for experimental synthesis and measurements to verify our strategy and calculations. This work demonstrates that the [VO_xS_{4-x}] (x = 0 - 4) tetrahedral groups are a good type of birefringent and NLO unit, but was long-termly overlooked, for the exploration of mid-IR NLO materials.

Table of Contents

Experimental Procedures

Single-crystal structure determination:

The Single-crystal structure determination was performed on Rigaku AFC10 diffractometer equipped with a graphite-monochromated Kα (λ = 0.71073 Å) radiation. A crystal of Na_3VOS_3 with a size of 0.15 × 0.2 × 0.2 mm^3 was picked for measurement. Diffraction data were collected using the Crystalclear software in the range of 3.4340° ≤ θ ≤ 28.725°, and the data was subjected to absorption correction using the XPREP program. The crystal structure framework is determined using the SHELEX direct method, with structure analysis and refinement carried out using SHELXS and OLEX2 software. Differential Fourier synthesis is used to determine the specific location of each atom. Finally, the coordinates and anisotropy parameters of all atoms are fitted by F2-based full matrix least squares fitting until the final convergence. The PLATON program was used to examine the symmetry of the structure, which revealed no high symmetry. As a result, the crystal structure of the compound was determined. Table S1 lists the data for structural refinement.

Reagents:

The following reagents used in the experiments were purchased directly from Aladdin Industries without further purification, including sodium sulphide (99.999%), vanadium (99.999%), vanadium pentoxide (99.99%), sulphur (99.99%).

Synthesis:

Polycrystalline powders of Na_3VOS_3 were obtained via high-temperature solid-state synthesis in an anhydrous and oxygen-free environment. The reagents were weighed and ground in stoichiometric ratios in a dry, inert argon glove box with oxygen and water vapour content below 0.1 ppm. The raw materials were sealed in quartz tubes under a high vacuum of 10^{-3} Pa and then placed in a temperature-programmed tube furnace. The quartz tubes were heated to 350°C at a rate of 13°C/h and maintained at this temperature for 100 hours. After the reaction, the tube furnace was turned off and allowed to cool naturally to room temperature.

Crystal Growth:

Single crystals of Na_3VOS_3 were grown using Li_2O as a flux and oxygen source. The reagent V: S: Li_2O: Na_2S was weighed to be 1: 5: 1.2: 2, fully ground, and packed into a quartz glass tube. The tube was then sealed in high vacuum and heated slowly to 450°C at a rate of 10°C/hour. The temperature was maintained at 450°C for 72 hours before being cooled to 100°C at a rate of 3°C/hour. Finally, the tube was naturally cooled to room temperature. After completion of the reaction, numerous red needle-like crystals adhered to the walls of the quartz tube. Cleaning the reaction products with DMF (Dimethyl Formamide) resulted in well-crystallized red needle-like crystals, some of which were up to a centimeter long. The crystal picture is shown in Figure 3b. The crystals are slightly deliquescent when left in the air for a long time.

Powder X-ray diffraction:

Polycrystalline Na_3VOS_3 powders were subjected to X-ray diffraction measurements using a Bruker D8 Focus powder diffractometer. The scanning range was 5° to 70° with a step length of 0.02° and a scanning speed of 0.1 s/step. The diffraction seam and the receiving seam were both 1.0 mm. The Cu target Kα radiation with a wavelength of λ= 1.5418 Å was used, and the operating voltage and current were 40 kV and 40 mA, respectively. The X-ray diffraction pattern agrees well with the fitted pattern of the solved Na_3VOS_3 crystal structure, indicating that a pure sample was obtained (Fig. 3a).

UV-vis-NIR diffuse reflectance spectra:

The Cary 7000 UV-vis-NIR spectrometer with diffuse integrating sphere attachment was used to collect the UV-vis-NIR diffuse reflection spectrum of Na_3VOS_3 powder at 298 K in the wavelength range of 200~2000 nm. With $BaSO_4$ as the reference material, the reflection spectrum was converted into the absorption spectrum through Kubelka-Munk function, from which one can obtain the experimental band gap of Na_3VOS_3

Power SHG measurement:

The Kurtz–Perry method was adopted to measure the SHG effect of Na_3VOS_3 powder. Standard sieve was use to divide the pure polycrystalline Na_3VOS_3 powder into five particle sizes (20-41 μm, 41–74 μm, 74–105 μm, 105–150 μm, 150–212 μm), which were used for test separately. The fundamental frequency light used in our measurement was generated by a Ho: Tm: Cr: YAG laser with a Q switch. The wavelength of the fundamental frequency light is 2090 nm (10 ns, 1 Hz). By measuring samples of different particle sizes, the relative intensities of the frequency doubling light and the fundamental frequency light were recorded on an oscilloscope. Ten values were taken for each particle size and averaged, and a reference material $AgGaS_2$ of comparable particle size was tested in the same way.

Energy-dispersive X-ray spectroscopy:

Semiquantitative EDS analyses were conducted using an energy-dispersive-X-ray (EDX)-equipped Hitachi S-4300 scanning electron microscope on the crystals that had been measured by single-crystal XRD.

Raman spectroscopy:

Raman spectroscopy was performed on inVia-Reflex instrument with a line of 532 nm of solid-state laser. The spectral range of the sample is between 100 and 800 cm^{-1}.

Photoluminescence measurements:

SUPPORTING INFORMATION

The photoluminescence spectra of Na_3VOS_3 were obtained using an inVia-Reflex Raman spectrometer from Renishaw, UK, by switching its regular operating mode.

Computational method:

First-principles calculations were performed on Na_3VOS_3 using the CASTEP package and the density functional plane-wave pseudopotential method.[1-3] Geometric optimization was carried out using the Broyden Fletcher Goldfarb Shanno (BFGS) minimization method.[4] The convergence criteria for energy, maximum force, maximum stress, and maximum displacement were set at 1×10^{-5}/eV, 0.03 eV/Å, 0.05 GPa and 10^{-3} Å, respectively. The local-density approximation (LDA) was chosen for all calculations. The plane wave cutoff energy[5] was set at 700 eV and the Monkhorst-Pack k point density in the Brillouin zone was set at 2x2x4. Norm-conserving pseudopotentials[6] were employed, with the valence electrons of Na $2s^22p^63s^1$,O $2s^22p^4$, S $3s^23p^4$, and V $3d^34s^2$.[7] As the exchange-correlation energy functional is discontinuous, LDA typically underestimates the band gap.[8] Therefore, a scissors factor correction was applied to calculate the optical properties. The SHG coefficient d_{ij} can be obtained by using the electron band structure modified by the scissors factor.[9] Additionally, a band-resolved d_{ij} and SHG density analysis is performed to demonstrate the SHG contributions of electronic orbitals and structural motifs in real space[10] To accurately evaluate the band gaps of the compounds, including the designed ones, we used the hybrid sx-LDA functionals.[11] The scissors factors of the designed compounds were set as the difference between the sx-LDA and LDA band gaps. According to our previous theoretical calculations, the parameter settings mentioned above can accurately predict the energy band gaps of chalcogenide compounds.[12, 13]

Results and Discussion


	wt%	at%
O	15.37	11.40
Na	31.65	37.72
S	35.51	38.60
V	17.47	12.28
Total:	100.00	100.00
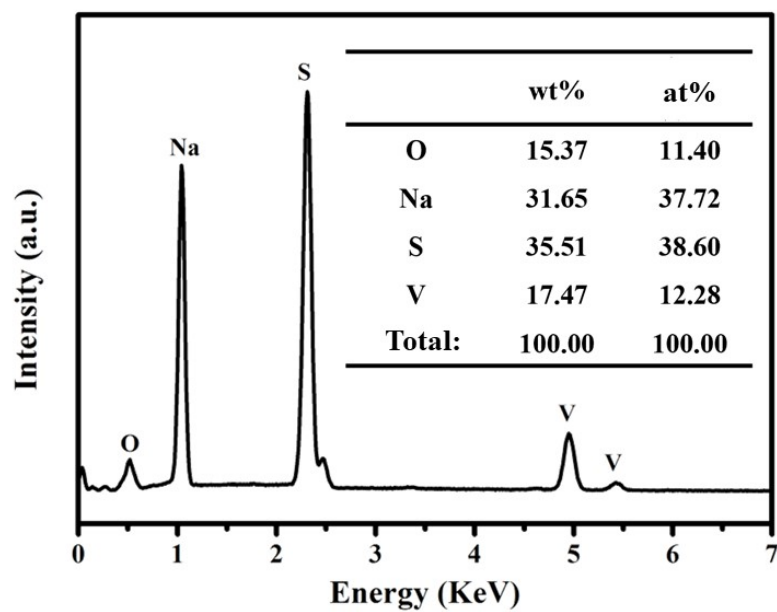
Figure S1. Energy dispersive spectrometer (EDS) image of Na_3VOS_3 crystal
The results showed a Na/V/O/S molar ratio of 3.3:1.1:3.3:1.0.
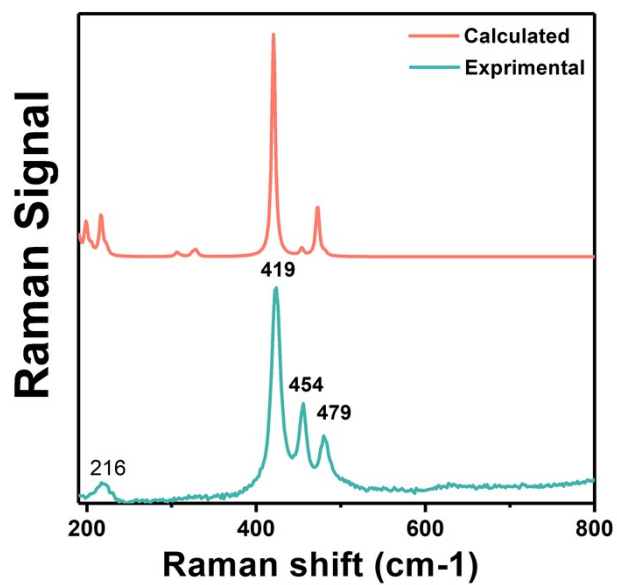
Figure S2. Comparison of the experimental raman spectra of Na_3VOS_3 and calculated spectra.

a_3VOS_3 exhibits significant absorption peaks at 216, 419, 454, and 479 cm^{-1}, which can be attributed to the characteristic absorption of the V-O bond, the respiratory vibration of the [VOS_3] tetrahedron, and the asymmetric stretching vibration, respectively.
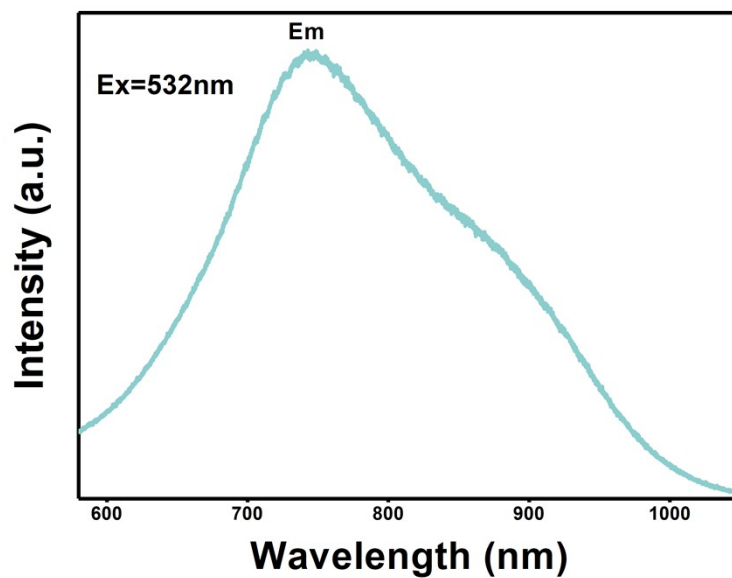
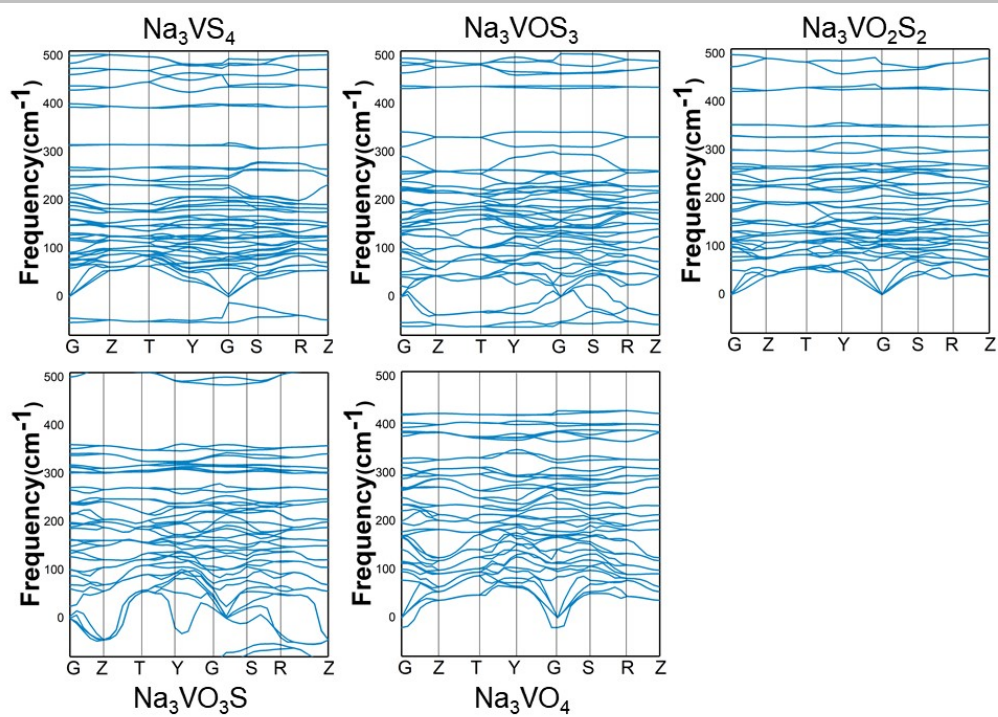**Figure S3.** Photoluminescence spectroscopy of Na_3VOS_3. The excitation light was set at 532 nm and the emission wavelength was measured to be around 710 nm.
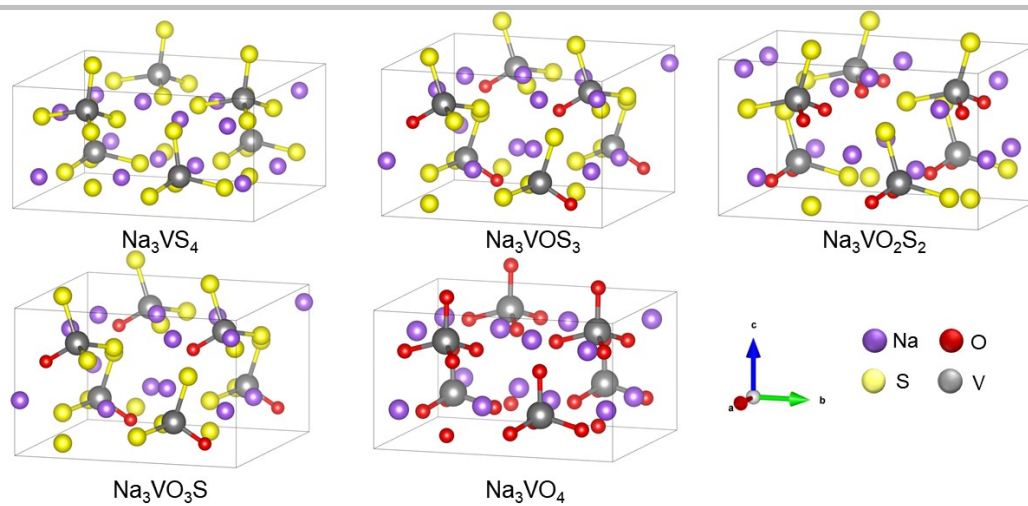
Figure S4. Designed a series $Na_3[VO_xS_{4-x}]$ (x = 0 - 4) compounds using β-Na_3VOS_3 as the parent structure.

Figure S5. calculated phonon spectra $Na_3[VO_xS_{4-x}]$ (x = 0 - 4)

Table S1. Δn and energy band gap data for tetrahedral sulfides, halides[14, 15]

Compounds	Eg	Δn @1µm	Compounds	Eg	Δn @1µm	Compounds	Eg	Δn @1µm
a-ZnS	3.24	0.000	Cu_2HgGeS_4	1.12	0.024	CuCl	2.600	0.000
b-ZnS	3.28	0.003	Cu_2ZnSnS_4	1.19	0.141	CuBr	2.700	0.000
$AgAlS_2$	3.18	0.047	$AgCd_2GaS_4$	2.32	0.059	CuI	3.300	0.000
$AgGaS_2$	2.76	0.034	$LiCd_2GaS_4$	2.61	0.017	CuI	3.400	0.013
$LiAlS_2$	4.68	0.014	$LiZn_2GaS_4$	3.1	0.017	LiI	6.200	0.013
$LiGaS_2$	3.77	0.014	$CuZn_2AlS_4$	2.12	0.006	ZnCl2-a	5.100	0.014
Ag_2GeS_3	1.45	0.092	$Ag_4CdGe_2S_7$	2.45	0.021	ZnCl2-b	5.000	0.029
Cu_2SiS_3	2.31	0.112	$Ag_4HgGe2S_7$	2.11	0.058	$CuGaCl_4$	3.800	0.005
Cu_2GeS_3	1.57	0.093	$Li_4CdGe_2S_7$	4.23	0.015	$CuAlCl_4$	4.600	0.000
Cu_2SiS_3	2.34	0.045	GeS_2	3.85	0.05	$CuAlBr_4$	4.400	0.000
Cu_2SnS_3	1.09	0.078	Ga_2S_3	3.01	0.041	$CuGaI_4$	3.200	0.002
Cu_3SbS_4	0.83	0.072	$HgGa_2S_4$	3.02	0.078	Cu_2HgI_4-a	2.500	0.032
Cu_3AsS_4	0.89	0.23	$CdGa_2S_4$	3.41	0.042	Cu_2HgI_4-b	2.000	0.024
Li_3PS_4	3.68	0.016	$ZnGa_2S_4$	3.6	0.029	Ag_2HgI_4-a	2.800	0.031
Cu_3PS_4	3.07	0.048	Hg_2SiS_4	2.92	0.118	Ag_2HgI_4-b	2.500	0.003
Ag_3PS_4	2.88	0.039	Hg_2GeS_4	2.8	0.096	Ag_2CdI_4	3.600	0.004
Li_2CdGeS_4	3.42	0.023	Hg_2SnS_4	2.4	0.022	Ag_2ZnI_4	3.700	0.022
Li_2CdSnS_4	3.11	0.018	Zn_2GeS_4	3.96	0.006			
a-Cu_2ZnSiS_4	2.01	0.052	$Zn_3(PS_4)_2$	3.19	0.035			
Li_2MnGeS_4	3.07	0.01	$InPS_4$	3.44	0.023			
a-Li_2MnSnS_4	3	0.011	$AlPS_4$	3.47	0.217			
Ag_2CdGeS_4	2.05	0.037	BPS_4	3.02	0.361			
Li_2ZnSnS_4	3.32	0.015	$LiZnPS_4$	3.76	0.072			
Ag_2ZnSiS_4	3.05	0.034	$AgZnPS_4$	3.21	0.051			
b-Cu_2ZnSiS_4	2.39	0.035	$LiBSiS_4$	3.87	0.03			
Cu_2CdSnS_4	1.05	0.134	$LiBGeS_4$	3.95	0.031			

9

SUPPORTING INFORMATION

Table S2. Representative works on photocatalytic methane coupling

Identification code	Na$_3$VOS$_3$
Empirical formula	Na$_2$O$_{0.67}$S$_2$V$_{0.67}$
Formula weight	154.73
Temperature/K	293(2)
Crystal system	orthorhombic
Space group	Cmc2$_1$
a/Å	9.5667(7)
b/Å	11.8659(9)
c/Å	5.8806(4)
α/°	90
β/°	90
γ/°	90
Volume/Å^3	667.55(8)
Z	6
Calculated density (g/cm^3)	2.309
Absorption coefficient (mm^{-1})	2.503
F(000)	448.0
2Θ range for data collection/°	6.868 to 57.45
Independent reflections	878 [R_{int} = 0.0735, R_{sigma} = 0.0469]
Final R indexes [I>=2σ (I)][a]	R_1 = 0.0331, wR_2 = 0.0842
Final R indexes [all data]	R_1 = 0.0345, wR_2 = 0.0853

$$_a R_1 = \sum ||F_0| - |F_c|| / \sum |F_0| \; for \; F_0^2 > 2\sigma(F_0^2). \; wR_2 = \{\sum [w(F_0^2 - F_c^2)^2] / \sum wF_0^4\}^{1/2} \; \text{for all date.} \; w^{-1} = \sigma^2(F_0^2) + (zP)^2, \text{where}$$

$$P = (Max(F_0^2, 0) + 2F_c^2)/3.$$

11

Table S3. Fractional atomic coordinates (×10^4) and equivalent isotropic displacement parameters (Å^2×10^3) for Na$_3$VOS$_3$. U$_{eq}$ is defined as 1/3 of of the trace of the orthogonalized U$_{IJ}$ tensor.

Atom	x	y	z	U(eq)
V001	5000	7980.4(6)	3468.5(19)	17.0(3)
S002	5000	6194.9(12)	2516(3)	26.9(4)
S003	6899.1(12)	8770.8(10)	2303.1(17)	29.3(3)
Na04	5000	6187(2)	7692(5)	30.6(6)
Na05	7054(2)	8805.9(18)	7507(4)	39.4(5)
O006	5000	8036(4)	6287(9)	27.3(11

Table S4. anisotropic displacement parameters ($Å^2 \times 10^3$) for Na_3VOS_3. The anisotropic displacement factor exponent takes the form:- $2\pi^2[h^2a^{*2}U_{11}+2hka^*b^*U_{12}+\ldots]$.

Atom	U_{11}	U_{22}	U_{33}	U_{23}	U_{13}	U_{12}
V001	21.4(4)	16.8(4)	12.9(4)	-0.3(4)	0	0
S002	37.9(8)	17.7(6)	25.0(7)	-2.9(5)	0	0
S003	25.3(5)	32.1(6)	30.4(7)	-0.8(4)	4.7(5)	-6.9(4)
Na04	40.4(15)	24.3(13)	27.0(14)	5.1(9)	0	0
Na05	37.2(11)	46.1(12)	34.9(12)	-0.3(9)	-5.7(10)	-7.7(8)
O006	39(3)	29(3)	15(2)	-0.2(15)	0	0

SUPPORTING INFORMATION

References

(1) Payne, M. C.; Teter, M. P.; Allan, D. C.; Arias, T. A.; Joannopoulos, J. D. Iterative minimization techniques for ab initio total-energy calculations: molecular dynamics and conjugate gradients. *Rev. Mod. Phys.* **1992**, *64* (4), 1045-1097. DOI: 10.1103/RevModPhys.64.1045.

(2) Kohn, W. Nobel Lecture: Electronic structure of matter---wave functions and density functionals. *Rev. Mod. Phys.* **1999**, *71* (5), 1253-1266. DOI: 10.1103/RevModPhys.71.1253.

(3) Clark, S. J.; Segall, M. D.; Pickard, C. J.; Hasnip, P. J.; Probert, M. I. J.; Refson, K.; Payne, M. C. First principles methods using CASTEP. *Z Krist-cryst Mater* **2005**, *220* (5-6), 567-570. DOI: doi:10.1524/zkri.220.5.567.65075 (acccessed 2022-08-25).

(4) Pfrommer, B. G.; Côté, M.; Louie, S. G.; Cohen, M. L. Relaxation of Crystals with the Quasi-Newton Method. *J. Comput. Phys.* **1997**, *131* (1), 233-240. DOI: https://doi.org/10.1006/jcph.1996.5612.

(5) Monkhorst, H. J.; Pack, J. D. Special points for Brillouin-zone integrations. *Phys. Rev. B* **1976**, *13* (12), 5188.

(6) Rappe, A. M.; Rabe, K. M.; Kaxiras, E.; Joannopoulos, J. Optimized pseudopotentials. *Phys. Rev. B* **1990**, *41* (2), 1227.

(7) Perdew, J. P.; Burke, K.; Ernzerhof, M. Generalized Gradient Approximation Made Simple. *Phys. Rev. Lett.* **1996**, *77* (18), 3865-3868. DOI: 10.1103/PhysRevLett.77.3865.

(8) Wang, C. S.; Klein, B. M. First-principles electronic structure of Si, Ge, GaP, GaAs, ZnS, and ZnSe. I. Self-consistent energy bands, charge densities, and effective masses. *Phys. Rev. B* **1981**, *24* (6), 3393-3416. DOI: 10.1103/PhysRevB.24.3393.

(9) Lin, J.; Lee, M. H.; Liu, Z. P.; Chen, C. T.; Pickard, C. J. Mechanism for linear and nonlinear optical effects in beta-BaB$_2$O$_4$ crystals. *Phys. Rev. B* **1999**, *60* (19), 13380-13389. DOI: 10.1103/PhysRevB.60.13380.

(10) He, R.; Lin, Z.; Lee, M.-H.; Chen, C. Ab initio studies on the mechanism for linear and nonlinear optical effects in YAl$_3$ (BO$_3$) $_4$. *J. Appl. Phys* **2011**, *109* (10), 103510.

(11) Bera, T. K.; Jang, J. I.; Song, J.-H.; Malliakas, C. D.; Freeman, A. J.; Ketterson, J. B.; Kanatzidis, M. G. Soluble semiconductors AAsSe$_2$ (A= Li, Na) with a direct-band-gap and strong second harmonic generation: a combined experimental and theoretical study. *J. Am. Chem. Soc.* **2010**, *132* (10), 3484-3495.

(12) Lin, Z. S.; Jiang, X. X.; Kang, L.; Gong, P. F.; Luo, S. Y.; Lee, M. H. First-principles materials applications and design of nonlinear optical crystals. *J Phys D Appl Phys* **2014**, *47* (25), 253001. DOI: 10.1088/0022-3727/47/25/253001.

(13) Kang, L.; Liang, F.; Jiang, X.; Lin, Z.; Chen, C. First-Principles Design and Simulations Promote the Development of Nonlinear Optical Crystals. *Acc. Chem. Res.* **2020**, *53* (1), 209-217. DOI: 10.1021/acs.accounts.9b00448.

(14) Liang, F.; Kang, L.; Lin, Z.; Wu, Y.; Chen, C. Analysis and prediction of mid-IR nonlinear optical metal sulfides with diamond-like structures. *Coord. Chem. Rev.* **2017**, *333*, 57-70. DOI: https://doi.org/10.1016/j.ccr.2016.11.012.

(15) Gong, P.; Liang, F.; Kang, L.; Lin, Z. Mid-Infrared Nonlinear Optical Halides with Diamond-like Structures: A Theoretical and Experimental Study. *Chem. Mater.* **2022**.

Author Contributions

P. G., Z. L. and L. D. conceived the project and designed the research.

S. Z. prepared and experimentally characterized Na$_3$VOS$_3$ samples. L. D. performed the density functional theory calculations. B. X., H. C., H. H., F. L., R. W. and P. G. provided assistance during the discussion of the results. L. D., P. G., and Z. L. wrote the manuscript. P. G., and Z. L. supervised the project. All the authors discussed the results and commented on the manuscript at all stages.